ELSEVIER

Journal of Neuroscience Methods xxx (2008) xxx–xxx

JOURNAL OF NEUROSCIENCE METHODS

www.elsevier.com/locate/jneumeth

Strain fields in histological slices of brain tissue determined by synchrotron radiation-based micro computed tomography

Marco Germann [a,b,c], Anne Morel [b], Felix Beckmann [d], Adrian Andronache [a], Daniel Jeanmonod [b], Bert Müller [a,c,*]

[a] *Computer Vision Laboratory, ETH Zürich, Sternwartstrasse 7, 8092 Zürich, Switzerland*
[b] *Department of Functional Neurosurgery, University Hospital Zurich, Sternwartstrasse 6, 8091 Zürich, Switzerland*
[c] *Biomaterials Science Center, University of Basel, c/o University Hospital Basel, 4031 Basel, Switzerland*
[d] *GKSS-Research Center, Max Planck-Str. 1, 21502 Geesthacht, Germany*

Received 30 August 2007; received in revised form 22 November 2007; accepted 2 January 2008

Abstract

Accurate knowledge of the morphology of the human brain is required for minimally or non-invasive surgical interventions. On the (sub-)cellular level, brain tissue is generally characterized using optical microscopy, which allows extracting morphological features with a wide spectrum of staining procedures. The preparation of the histological slices, however, often leads to artifacts resulting in imperfect morphological data. In addition, the generation of 3D data is time-consuming. Therefore, we propose synchrotron radiation-based micro computed tomography (SRμCT) avoiding preparation artifacts and giving rise to the 3D morphology of features such as gray and white matter on the micrometer level. One can differentiate between white and gray matter without any staining procedure because of different X-ray absorption values. At the photon energy of 10 keV, the white matter exhibits the absorption of 5.08 cm^{-1}, whereby the value for the gray matter corresponds to 5.25 cm^{-1}. The tomography data allow quantifying the local strains in the histological images using registration algorithms. The deformation of histological slices compared to the SRμCT in a 2D–2D registration leads to values of up to 6.3%. Mean deformation values for the Nissl-stained slices are determined to about 1%, whereas the myelin-stained slices yield slightly higher values than 2%.

Keywords: Brain tissue; 3D visualization; Synchrotron radiation; X-ray absorption; Image registration; Histological strain

1. Introduction

Non-invasive magnetic resonance (MR)-guided neurosurgery without intracerebral penetration such as with gamma knife or high-intensity focused ultrasounds (Jolesz et al., 2005; Keep et al., 2005; Kennedy et al., 2003; Ohye et al., 2005; Young, 2002) represents an alternative to deep brain stimulation (DBS) or radiofrequency lesions. The location of the target volume, e.g. in the thalamus, with desired precision becomes possible even if the target is not identifiable on the acquired MR-images, using a detailed generic atlas of the human thalamus (Morel, 2007; Morel et al., 1997; Niemann et al., 2000). The applications of the atlas and prior knowledge to the actual therapy require, however, specific approaches. The current planning of the neurosurgical intervention, which basically relies on fixed spatial relations between target volume and different anatomical landmarks, can be meaningfully enhanced and generalized, taking into account the variability of the different anatomical structures of interest. Here, the important task is to establish the anatomically meaningful correspondence between the features in the training set and those specific to the patient (Davies et al., 2002; Styner et al., 2003). Due to the complexity of the model and the unknown deficiencies in slice preparation, the relative positioning of the differently stained histological slices belongs to the major challenges when building a statistical shape model. Known algorithms permit to fit the average model to the actual patient-specific MRI data, cp., e.g. van den Elsen et al. (1993).

The morphology of human tissue, as for the generic thalamic atlas, is generally characterized on sub-micrometer level using optical microscopy techniques. The techniques are based on

* Corresponding author at: Biomaterials Science Center, University of Basel, c/o University Hospital Basel, 4031 Basel, Switzerland. Tel.: +41 61 265 9660; fax: +41 61 265 9699.
E-mail address: bert.mueller@unibas.ch (B. Müller).

0165-0270/$ – see front matter © 2008 Elsevier B.V. All rights reserved.
doi:10.1016/j.jneumeth.2008.01.011

histological sectioning with section thickness of several 10 μm. The preparation procedure leads to stress and strain of the anisotropic and inhomogeneous soft matter and finally leads to deformations, which are expected to be critical for mellow tissue including brain segments. In creating a brain atlas for MR-guided neurosurgery, non-rigid or elastic transformations are commonly used to correct for spatial distortion occurring during brain preparation (Chakravarty et al., 2006; Mazziotta et al., 2001). In absence of *in vivo* MRI from the same brain, the differential distortion factors intervening during brain extraction, fixation and histological processing cannot be precisely evaluated, but significant, variable 2D distortions appear to occur during sectioning and histological processing (Lang, 2006; Mai et al., 2004; Yelnik et al., 2007). In spite of increasing MR imaging resolution, particularly from postmortem material, it is still insufficient for accurate delimitation of structures of interest such as individual thalamic nuclei (Deoni et al., 2005; Fatterpekar et al., 2003; Pfefferbaum et al., 2004). In this context, the possibility to obtain a high-resolution 3D representation of the brain segment for correcting the local deformations is particularly relevant for atlas-to-MR registration and therefore for targeting in MR-guided non-invasive functional neurosurgery.

Synchrotron radiation-based micro computed tomography (SRμCT) as a non-destructive technique provides the necessary spatial and to some extent, also, density resolution. The difference in the X-ray absorption of gray and white matter can be calculated using published data of density and chemical composition (Brooks et al., 1980). For the photon energy of 80 keV it is found that the difference is about 6% after removing the Compton scattering component (Brooks et al., 1980). The removal of Compton scattering, however, is experimentally impossible and, hence, this difference is just a several tenths of a percent. The decrease of photon energy to 10 keV improves the contrast by more than one order of magnitude. Therefore, it might be advantageous to use monoenergetic photons of about 10 keV. Because of the high intensity provided at the synchrotron radiation sources, a monochromator can be inserted to realize a tunable X-ray source. Here, the beam hardening is drastically reduced. Furthermore, the Gaussian shape of the absorption histograms allows for intensity-based thresholding in many cases (Müller et al., 2002). It has to be mentioned that the photoelectric absorption of brain and water is very similar, which makes differentiation of brain in water difficult. The situation becomes even more difficult if phosphate buffer is used instead of water. Consequently, successful measurements in wet environment, although desirable to avoid shrinking artifacts, are more demanding.

The value of the tomograms of brain matter lies especially in the 3D information, which offers the possibility to elastically register the sets of histological slices by means of these less-detailed 3D data. The brain tissue belongs to the inhomogeneous, deformable tissues that change their shape caused by intrinsic stress relaxation or externally applied forces. The geometrical expression of these deformations is termed strain and defined as the length change related to the original length. In the case of anisotropic and inhomogeneous medium (brain tissue) one has to consider the strain at the different points in 3D space. Mathematically represented as the tensor field, one may use for the representation of the local strains the terms strain tensor and *strain field*. The combination of the different information at the micrometer and millimeter scales obtained from histology and SRμCT offers a promising tool to significantly improve the accuracy of the generic brain atlas.

2. Materials and methods

For the experiments, small blocs of the rostral medulla oblongata including parts of the inferior olivary nucleus were dissected from a normal human brain with no neuropathological signs at autopsy. The brain had been fixed in 10% formalin for 10 years. The blocs were cut to the length of about 6 mm and the diameter of 4 mm. These blocs were placed in 0.5-ml Eppendorf tubes filled with 0.1 M phosphate buffer (PB). They were kept in the Eppendorf tubes at the temperature of 4 °C for transportation. The SRμCT measurements performed at HASYLAB at DESY, Hamburg, Germany, were carried out at room temperature within about 8 h. After these measurements, the brain samples in the Eppendorf tubes were cryo-protected in sucrose (20% solution in PB) for 2 weeks, before they were frozen and stored (−75 °C). For histology, 30-μm sections were cut in the cryostat and collected in PB before they were mounted on gelatinized glass slides. Two series of sections were stained for Nissl (with cresyl-violet) or for myelin with a modified Heidenhain–Woelcke procedure applied to the mounted sections (Bürgel et al., 1997). The sections were examined under a Leica microscope (MZ 16) and photographed with a digital camera (DLC 420C).

The 3D morphology of different kinds of biological matter such as human brain tissue can be quantitatively characterized with true micrometer resolution using SRμCT in absorption contrast mode. The main advantage with respect to conventional μCT is the much higher photon flux, offering to eliminate all X-ray photons but the ones of selected energy, and still maintain a reasonable acquisition time. Bragg reflection at single crystals permits the selection of the photon energy with the precision of 10^{-4}. The attenuation coefficient μ of brain tissue depends strongly on the photon energy E, which can be optimized by the relation $\mu(E, Z)D = 2$ (Grodzins, 1983), where D corresponds to the average sample diameter and Z to the atomic number of the related element. Accordingly, we selected the photon energy of 10 keV for the present study. The spatial resolution was determined by the modulation transfer function of a gold plate edge recorded under the conditions applied for the data acquisition (Müller et al., 2001). It corresponds to 6.20 μm for the present study. Note, the voxel size was chosen to 4.05 μm before binning.

The SRμCT setup is schematically given in Fig. 1. The experiments were carried out at the beamline BW 2 (HASYLAB at DESY, Hamburg, Germany) taking advantage of the absorption contrast tomography (Beckmann, 2002). Positrons with the energy of 4.5 GeV are forced to travel along the curved path by the bending magnets of the storage ring DORIS III. The wiggler of the beamline BW 2 is a magnetic structure of 28 periods to generate the necessary photon flux. The fixed exit double crystal monochromator, Si(1 1 1) provides the monochromatic X-ray beam of selected energy and flux. The sagittal-bent sec-

Please cite this article in press as: Germann M, et al., Strain fields in histological slices of brain tissue determined by synchrotron radiation-based micro computed tomography, J Neurosci Methods (2008), doi:10.1016/j.jneumeth.2008.01.011

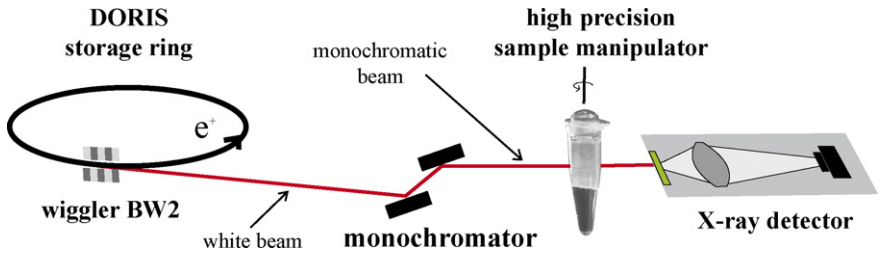

Fig. 1. For the SRμCT measurements, the small bloc of brain tissue placed in an Eppendorf tube is mounted on the high-precision sample manipulator at the beamline BW 2 (HASYLAB at DESY, Hamburg, Germany). This setup operated by the GKSS-Research Center allows using a monochromatic X-ray beam of selected energy and to rotate the sample in parts of a degree. For the 3D representation of the brain sample, 721 projections were detected.

ond Si(1 1 1) crystal reduces the beam divergence and forms a parallel beam about 10-mm wide and 3-mm high. This beam hits the sample at a certain angle and generates the related projection image on the fluorescence screen, which was a 1-mm thick $CdWO_4$ single crystal. After moderate magnification, this optical image is mapped on a Kodak KAF 1600 CCD-chip (1536×1024 pixels, pixel length 9 μm) and acquired using 14-bit digitalization at the frequency of 1.25 MHz. The sample manipulator allows the precise specimen positioning and rotation. For the present study, four datasets at different sample heights, shifted by 1.5 mm, each with 721 projections were acquired by rotating the sample in steps of 0.25° from 0° to 180°. In order to eliminate the beam non-uniformities and account for the detector noise, the difference between the individual bare projections and the dark image was divided by the difference of the beam and the dark image to obtain the corrected projections, which were the basis of the reconstruction. Nevertheless, image non-uniformities still existed due to the photon counting statistics and defects in the fluorescence screen.

The data from the SRμCT measurements were reconstructed slice-by-slice with the filtered back-projection algorithm (Kak and Slaney, 1988). Before reconstruction, the data were binned by the factor 3 to improve the density resolution reducing the spatial resolution (Thurner et al., 2004). The voxel size after binning is, therefore, 12.16 μm. Note that the number of photons counted per pixel increases by the square of the binning factor, which finally increases the contrast between the different morphological features identified, considerably.

The SRμCT data served for the determination of the local absorption values with the aim to discriminate between characteristic features of the tissue. The comparison with the related histological slices should allow quantifying the deformation produced as the result of the preparation processes of the slices. For the evaluation of the local absorption of the brain tissue, namely the inferior olivary nucleus, which consists of gray and white brain matter, the different parts including the surrounding phosphate buffer have to be segmented. Because of the similar absorption values, the segmentation cannot be performed in a fully automatic fashion. Therefore, we have manually selected representative areas in 30 SRμCT slices with a total volume of about 200,000 voxels. This selection is shown for one slice in Fig. 2. Since the blood vessels are expected to be filled with PB, they were excluded from our analysis.

In order to determine the strain of the histological slices one has to register them with the related SRμCT slices by means

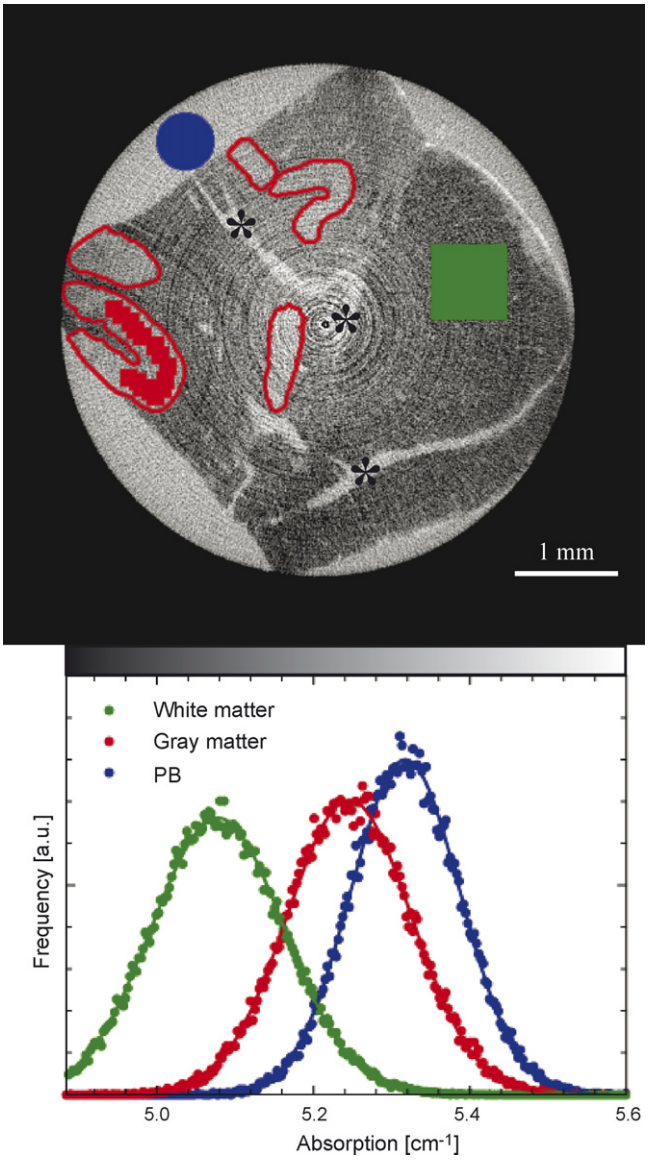

Fig. 2. On the SRμCT slice the gray matter (bordered in red) and blood vessels (*) can be distinguished from the surrounding white matter. The opaque fields demonstrate the manual segmentation of phosphate buffer (blue), white matter (green) and gray matter (red) for the calculation of the related X-ray absorption values. The absorption value histograms obtained from the different selected areas are given in the indicated color index. They are described by Gaussians.

Please cite this article in press as: Germann M, et al., Strain fields in histological slices of brain tissue determined by synchrotron radiation-based micro computed tomography, J Neurosci Methods (2008), doi:10.1016/j.jneumeth.2008.01.011

of an elastic registration algorithm. The registration algorithm chosen (Andronache, 2006) is based on the adaptive hierarchical image subdivision strategy, which decomposes the non-rigid matching problem into numerous local rigid registrations of sub-images of decreasing size. Because of the different nature of image modalities, the local registrations were performed using the classical maximization of Mutual Information (MI) principle (Viola and Wells, 1995; Maes et al., 1996). The local registration parameters are found using the Powell multi-dimensional search algorithm (Press et al., 1988) such that the MI between the reference μCT and the floating histological sub-images is maximized. The hierarchical image splitting strategy was proposed by Likar and Pernus (2001) and using several improvements recently extended to 3D (Andronache et al., 2008). The hierarchical splitting is governed by a sub-image information consistency test in the form of the Moran spatial autocorrelation coefficient. At each level of the hierarchy, the consistency of the information contained in each of further sub-divided images is tested, and all those sub-images failing this test being no longer subdivided or registered at the successive levels. This consistency test is also used as the stopping criterion for the entire registration algorithm. The hierarchical image subdivision is complete when no structural information is found in any of the currently partitioned sub-images, and therefore, their local registration is meaningless. As a consequence of the use of the information consistency test, at the last hierarchical level, the size of the sub-images may differ from one another. A typical minimum size is around 8×8 pixels depending on the level of details and noise in the original image. The final deformation field is estimated from all the registration parameters of all the sub-images at the last hierarchical level by thin plate splines (TPS) interpolation. Because of the missing ground truth for the problem here, one cannot provide the validation of the registration result for the particular case. In another case (Andronache, 2006), however, this registration method was validated. The registration errors were estimated with real data of known deformation field. More precise, using an MR scanner, T1 and T2 images of the liver were acquired simultaneously at different stages of the respiratory cycle. The non-rigid registration was then used to recover the deformation fields, and the statistics led to an accuracy of 1.07 ± 0.75 in pixel dimensions.

To simplify matters, for each histological slice the related SRμCT slice was manually selected. These two slices of different modalities underwent the registration in 2D fashion.

3. Results

Fig. 2 shows that SRμCT measurements performed at the photon energy of 10 keV allows for the differentiation of gray and white matter in PB. The quantitative evaluation based on selected images provides the expected Gaussians in the absorption histograms. The parameters of these Gaussians are the amplitude, i.e. the number of voxels included, the half-width, and the absorption values. The normalized Gaussians are presented in Fig. 2 (bottom) in order to demonstrate that even the simple intensity-based segmentation by means of a threshold, chosen by the crossing points of the Gaussians, enable us to successfully differentiate between white and gray matter in water in an automatic way. The differentiation between gray matter and PB, however, is much more difficult because of the strong overlap in the absorption values. Nevertheless, after binning with a factor of 3 the contrast is high enough to register the histological data with the tomographic slices.

For the white matter, the absorption value is $5.078\,\mathrm{cm}^{-1}$. The gray matter has an absorption value of $5.246\,\mathrm{cm}^{-1}$. The value for PB is only slightly higher namely $5.318\,\mathrm{cm}^{-1}$. Hence the absorption of the gray matter is just 3.2% larger than that of white matter. The half-width is almost constant for the three peaks and corresponds to $(0.08 \pm 0.01)\,\mathrm{cm}^{-1}$.

Figs. 3 and 4 show how the differently stained histological sections and the related SRμCT slices differ. For each sample the rigid (top right) and the non-rigid registration (bottom left) based on the SRμCT-data are presented. The non-rigid registration emerges from the rigidly registered slice. Therefore, the differences between the non-rigidly registered slice and the rigidly registered one illustrate the local deformations caused by the different preparation steps of the tissue for histology. The arrows in Figs. 3 and 4 (bottom right) quantitatively characterize these deformations. The average extension or mean absolute strain (arrow length) in the Nissl-stained slice is 55.9 μm. The one of the myelin-stained slice is almost doubled, namely 109.2 μm. In order to extract a more general quantity the (relative) strain is considered. The local extensions or the absolute strains have to be related to the slice extension as original length. As the lower limit of the slice extension one may apply the smallest diameter of the circle that fully includes the entire slice. This choice leads to 0.99% for the Nissl-stained sample and to 1.90% for the myelin-stained sample. Using the largest circle to be fully incorporated into the slice one obtains the upper limit of the slice extension. This limit gives rise to only slightly higher values. They correspond to 1.32% for the Nissl-stained and to 2.51% for the myelin-stained slices.

These average relative strain values are, however, only of minor interest since they may significantly depend on the slice dimensions and other specific approaches in the preparation process. The maximal strain, which is related to the longest arrow, belongs to the quantities that are fundamental for the development of a precise brain atlas. According to the definitions given above, the maximal strain for the Nissl-stained slices is between 7.0% and 9.3%. The values for the myelin-stained slices lie between 11.6% and 15.2%.

4. Discussion

Histological sectioning is generally used to characterize brain tissue with high lateral spatial resolution. The preparation of the histological slices leads, however, to tissue deformations, which depend on the staining and mounting procedures. Commonly, one expects local strains of a few percents, which seem to be tolerable. The actual strain values, however, are unknown. Distortions occurring prior to histological processing, i.e. during brain extraction and fixation, are difficult to estimate in absence of *in vivo* imaging. Limited deformations of gray and white matter seem to occur with formalin fixation (Lang, 2006), par-

Please cite this article in press as: Germann M, et al., Strain fields in histological slices of brain tissue determined by synchrotron radiation-based micro computed tomography, J Neurosci Methods (2008), doi:10.1016/j.jneumeth.2008.01.011

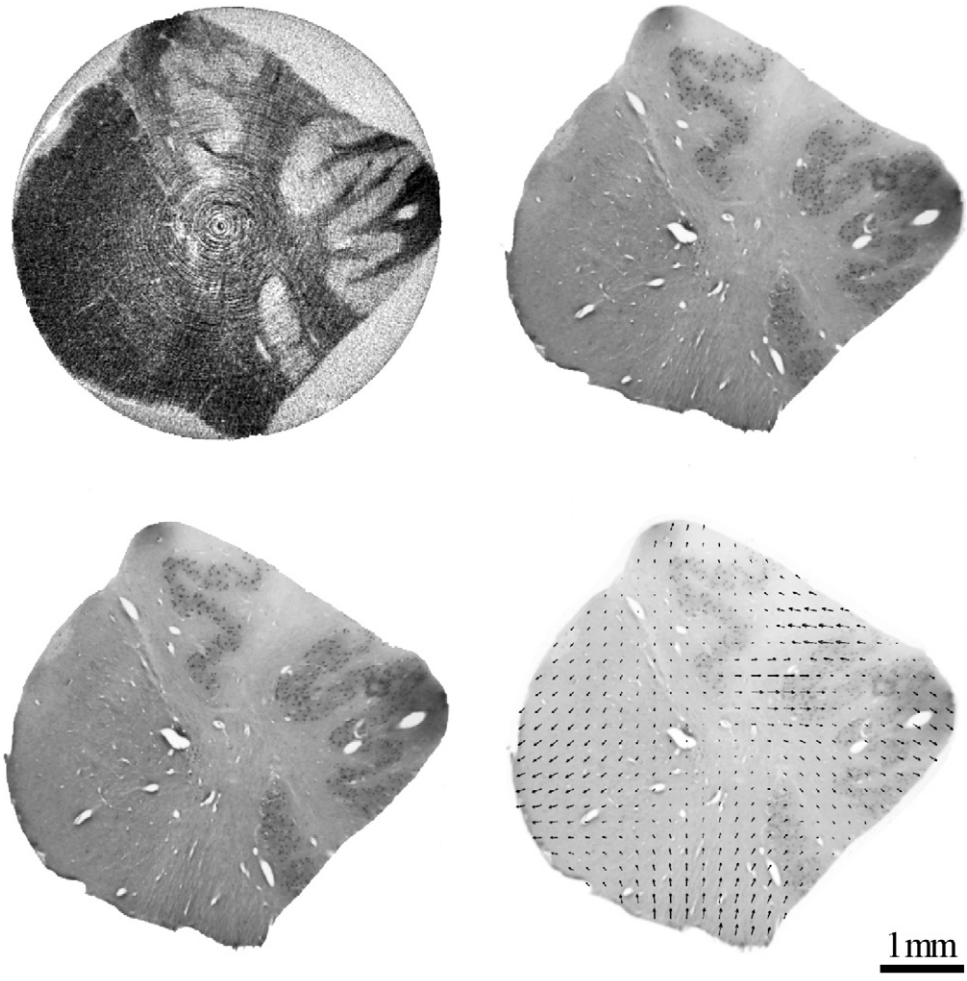

Fig. 3. A Nissl-stained section is rigidly registered (top right) to the related SRμCT-slice (top left). Since human brain tissue deforms due to the mechanical stress during the preparation, a non-rigid registration (bottom left) is applied. The direction and amplitude of strain fields (local deformations) are presented with black arrows (bottom right).

ticularly for central structures such as the thalamus. The overall shrinkage factors evaluated after short fixation times and by comparison between postmortem MRI and stained cryo-sections were minimal in the section plane but detectable for distances measured across sections (1.12%) (Morel, 2007). Therefore, it is attractive to search for techniques that enable us to determine the local strains in order to allow correcting the related preparation artifacts.

Micro computed tomography based on X-rays permits the 3D visualization of tissue in wet environment, i.e. of brain tissue before sectioning in a non-destructive manner. Although it is possible to discriminate between gray and white matter (Brooks et al., 1980), the difference in contrast is so small that often only the mean values are considered (Hubbell and Seltzer, 2007). The present study was performed at the synchrotron radiation source and not by means of a conventional X-ray source to uncover the inferior olivary nucleus within the rostral medulla oblongata and the blood vessels filled with phosphate buffer with better density resolution on the micrometer scale.

The contrast between white and gray matter in computed tomography is explained by the different chemical composition (Brooks et al., 1980). It gives rise to significantly different photoelectric X-ray absorption. Based on the data given by Brooks, one can estimate this difference for the photon energy of 10 keV and obtains 5.6%. Consequently, the measurement that yielded 3.2% is reasonable especially since the tissue preparation is likely to be different. Note that the measured value for the X-ray absorption of PB is just 4″ higher than the simulated one indicating appropriate calibration of the SRμCT setup.

Because of the different X-ray absorption rates within the white and the gray matter, the SRμCT data clearly delineates the two tissues, making possible the registration of the histological slices. However, as the SRμCT data is a 3D volume while the histological slice is a 2D image, serious problems may be encountered because of the large number of degrees of freedom of such a non-rigid 2D–3D registration. Therefore, in general, no unique solution is found. Extracting a region of interest, where the histological slice is cut out, the degrees of freedom are meaningfully reduced. As the limit, one might restrict the region of interest to a single tomographic slice resulting in the non-rigid 2D–2D registration algorithm. As a first step such a restriction is rather simple, because one can recognize many individual features including outer shape, vessels, and nuclei. Such a procedure is a simplification of the original task and decreases the

Please cite this article in press as: Germann M, et al., Strain fields in histological slices of brain tissue determined by synchrotron radiation-based micro computed tomography, J Neurosci Methods (2008), doi:10.1016/j.jneumeth.2008.01.011

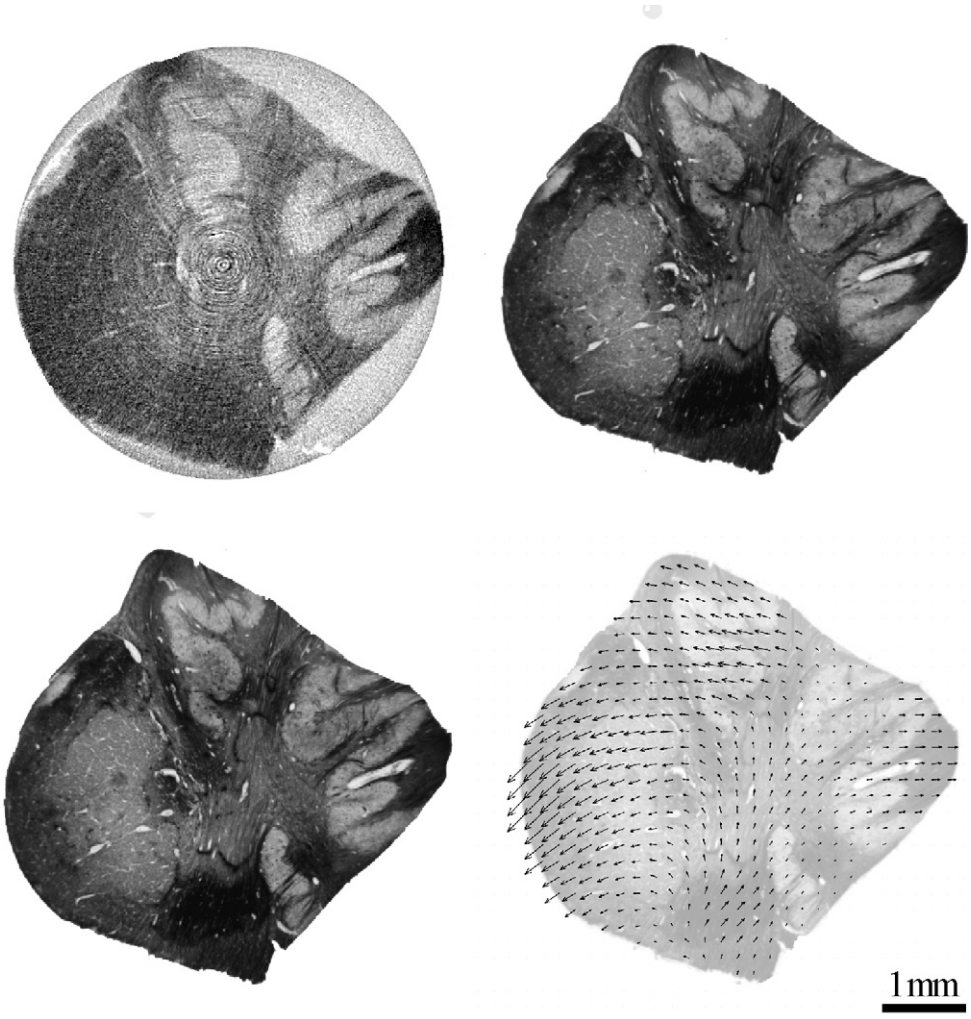

Fig. 4. The registration of the myelin-stained section to the related SRμCT slice shows much larger deformations than for the Nissl-stain (cp. Fig. 3). The conventions are identical to Fig. 3.

accuracy of the strain data. However, the visual inspection of the features in the tomographic slices above and below the selected one indicates that this effect can be neglected. It should be noted that any desired plane can be extracted from the SRμCT as it provides 3D data non-destructively, and further used for the non-rigid 2D–2D registration.

The strain values determined show that the preparation procedure of Nissl-staining leads to only about 50% of the one for the myelin stain. Although the sections were mounted similarly prior to staining in the two procedures, the longer time in the staining solution, which also contains some alcohol, may explain the higher strain value for myelin-stained sections (Bürgel et al., 1997).

The specimen's diameter selected (4 mm) is rather small. It is, however, not a restriction, because the X-ray beam at the beamline BW 2 can be increased to about 20 mm. Using the beamline W 2 (HARWI) at HASYLAB at DESY one can even reach beam widths of 70 mm. In addition, one can set the rotation axis asymmetric to the beam and rotate the specimen by 360° to acquire tomograms of specimens with diameters up to the double beam width (Müller et al., 2007). In order to keep the spatial resolution for the visualization of larger specimens constant, one has to reduce the rotation angle increment and to increase the number of pixels in the acquired images. Both changes are possible from an experimental point of view and just increase the data size. The main restriction results from the energy dependence of the attenuation coefficient $\mu(E)$. Following the relation $\mu(E)D = 2$ (Grodzins, 1983), the SRμCT of larger samples correlates with higher photon energies. At these higher photon energies the contrast between white and gray matter becomes weaker. Consequently, the method proposed will work for the entire thalamus but might become impossible for the brain as a whole. Please note that histology is often not performed for specimens larger than the thalamus diameter.

Functional neurosurgery requires the determination of the exact position of the target. Although the SRμCT data presented here are on rather small brain specimens, the application of the technique to larger blocks, such as the entire thalamus, will allow the more precise positioning of the desired structure even if

Please cite this article in press as: Germann M, et al., Strain fields in histological slices of brain tissue determined by synchrotron radiation-based micro computed tomography, J Neurosci Methods (2008), doi:10.1016/j.jneumeth.2008.01.011

the limits are invisible in pre-operative MRI and thus offer an additional tool for clinical application.

Acknowledgements

The authors thank V. Streit and J. Liu for histological work. The study has been partially supported by the National Center of Competence in Research (NCCR) 'Computer aided and image guided medical interventions' (Co-Me) funded by the Swiss National Science Foundation. Beamtime at the beamline BW 2 (HASYLAB at DESY) was allocated within the proposal II-20060035 EC.

References

Andronache A, Multi-modal non-rigid registration of volumetric medical images. In: Information technology and electrical engineering, Zürich No. 16601: Zürich: ETH; 2006.

Andronache A, von Siebenthal M, Székely G, Cattin P. Non-rigid registration of multi-modal images using both mutual information and cross-correlation. Med Image Anal 2008;12:3–15.

Beckmann F. Microtomography using synchrotron radiation as a user experiment at beamlines BW2 and BW5 of HASYLAB at DESY. In: Bonse U, editor. Developments in X-ray tomography III, vol. 4503. San Diego, USA: SPIE; 2002. p. 34–41.

Brooks RA, Di Chiro G, Keller MR. Explanation of cerebral white–gray contrast in computed tomography. J Comput Assist Tomogr 1980;4:489–91.

Bürgel U, Mecklenburg I, Blohm U, Zilles K. Histological visualization of long fiber tracts in the white matter of adult human brains. J Hirnforschung 1997;38:397–404.

Chakravarty MM, Bertrand G, Hodge CP, Sadikot AF, Collins DL. The creation of a brain atlas for image guided neurosurgery using serial histological data. Neuroimage 2006;30:359–76.

Davies RH, Twining DJ, Cootes TF, Waterton JC, Taylor CJ. A minimum description length approach to statistical shape modeling. IEEE TMI 2002;21:525–37.

Deoni SC, Josseau MJ, Rutt BK, Peters TM. Visualization of thalamic nuclei on high resolution, multi-averaged T1 and T2 maps acquired at 1.5 T. Hum Brain Mapp 2005;25:353–9.

Fatterpekar GM, Delman BN, Boonn WW, Gultekin SH, Fayad ZA, Hoff PR, et al. MR microscopy of normal human brain. Magn Reson Imaging Clin N Am 2003;11:641–53.

Grodzins L. Optimum energies for X-ray transmission tomography of small samples. Nucl Instrum Methods 1983;206:S41–5.

Hubbell JH, Seltzer SM. Tables of X-ray mass attenuation coefficients and mass energy-absorption coefficients. NIST; 2007.

Jolesz FA, Hynynen K, McDannold N, Tempany C. MR imaging-controlled focused ultrasound ablation: a noninvasive image-guided surgery. Magn Reson Imaging Clin N Am 2005;13:545–60.

Kak AC, Slaney M. Principles of computerized tomographic imaging. New York: IEEE Press; 1988.

Keep MF, Mastrofrancesco L, Erdman D, Murphy B, Ashby LS. Gamma knife subthalamotomy for Parkinson disease: the subthalamic nucleus as a new radiosurgical target—case report. J Neurosurg 2005;97:592–9.

Kennedy JE, Ter Haar GR, Cranston D. High intensity focused ultrasound: surgery of the future? Br J Radiol 2003;76:590–9.

Lang G. Histotechnik: Praxislehrbuch für die Biomedizinische Analytik. Wien: Springerverlag; 2006.

Likar B, Pernus F. A hierarchical approach to elastic registration based on mutual information. Image Vision Comput 2001;19:33–44.

Maes F, Collignon A, Vandermeulen D, Marchal G, Suetens P. Multi-modality image registration by maximation of mutual information. In: Mathematical methods in biomedical image analysis. IEEE; 1996. p. 14–22.

Mai JK, Assheuer J, Paxinos G. Atlas of the human brain. 2nd ed. San Diego: Elsevier Academic Press; 2004.

Mazziotta J, Toga A, Evans A, Fox P, Lancaster J, Zilles K, et al. A four-dimensional probabilistic atlas of the human brain. J Am Med Inform Assoc 2001;8:401–30.

Morel A. Stereotactic atlas of the human thalamus and basal ganglia. New York: Informa Healthcare USA, Inc; 2007.

Morel A, Magnin M, Jeanmonod D. Multiarchitectonic and stereotactic atlas of the human thalamus. J Comp Neurol 1997;387:588–630.

Müller B, Thurner P, Beckmann F, Weitkamp T, Rau C, Bernhardt R, et al. Non-destructive three-dimensional evaluation of biocompatible materials by microtomography using synchrotron radiation. In: Bonse U, editor. Developments in X-ray tomography III, vol. 4503. San Diego, USA: SPIE; 2001. p. 178–88.

Müller B, Beckmann F, Huser M, Maspero F, Székely G, Ruffieux K, et al. Non-destructive three-dimensional evaluation of a polymer sponge by microtomography using synchrotron radiation. Biomol Eng 2002;19:73–8.

Müller B, Bernhardt R, Weitkamp T, Beckmann F, Bräuer R, Schurigt U, et al. Morphology of bony tissues and implants uncovered by high-resolution tomographic imaging. Int J Mater Res 2007;98:613–21.

Niemann K, Mennicken V, Jeanmonod D, Morel A. The Morel stereotactic atlas of the human thalamus: atlas-to-MR registration of internally consistent canonical model. Neuroimage 2000;12:601–16.

Ohye C, Shibazaki T, Sato S. Gamma knife thalamotomy for movement disorders: evaluation of the thalamic lesion and clinical results. J Neurosurg 2005;102(suppl.):234–40.

Pfefferbaum A, Sullivan EV, Adalsteinsson E, Garrick T, Harper C. Postmortem MR imaging of formalin-fixed human brain. Neuroimage 2004;21:1585–95.

Press WH, Flannery BP, Teukolsky SA, Vetterling WT. Numerical recipes in C—the art of scientific computing. Cambridge University Press; 1988.

Styner MA, Rajmani KT, Nolte L-P. Evaluation of 3D correspondence methods for model building. Proc IPMI 2003:63–75.

Thurner P, Beckmann F, Müller B. An optimization procedure for spatial and density resolution in hard X-ray micro-computed tomography. Nucl Instrum Methods 2004;225:599–603.

van den Elsen PA, Pol EJD, Viergever MA. Medical image matching—a review with classification. IEEE Eng Med Biol 1993;12:26–39.

Viola P, Wells WM. Alignment by maximation of mutual information. In: Proceedings of the fifth international conference on computer vision; 1995.

Yelnik J, Bardinet E, Dormont D, Malandain G, Ourselin S, Tande D, et al. A three-dimensional, histological and deformable atlas of the human basal ganglia. I. Atlas construction based on immunohistochemical and MRI data. Neuroimage 2007;34:618–38.

Young RF. Gamma knife radiosurgery as an alternative form of therapy for movement disorders. Arch Neurol 2002;59:1660–2 [author reply 2–4].

Please cite this article in press as: Germann M, et al., Strain fields in histological slices of brain tissue determined by synchrotron radiation-based micro computed tomography, J Neurosci Methods (2008), doi:10.1016/j.jneumeth.2008.01.011